Journal of Materials and Electronic Devices 2 (2021) 12-18

Magnetic and Structural Characterization of Inorganic/Organic coated Fe_3O_4 Nanoparticles

Nurdan Kurnaz Yetim[1*], Fatma Kurşun Baysak[1]

[1]Kırklareli University, Faculty of Arts and Sciences, Department of Chemistry, Kırklareli, Turkey

Metal nanoparticles have the potential to be used in many technological and medical applications, especially in imaging, diagnosis, and treatment. Most of the metal nanoparticles are cytotoxic. Coating of metal nanoparticles with inorganic / organic groups is proposed to reduce their toxicity. In our research, Fe_3O_4 nanoparticles were produced by the co-precipitation method and separately coated with tetraethyl orthosilicate (TEOS), polyethylene glycol (PEG) and chitosan molecules in order to reduce their cytotoxicity where core@shell magnetic nanostructures were obtained. For the chemical characterization of the coated magnetic nanoparticles, Fouirer Transform Infrared (FTIR) spectra were taken, and thermal gravimetric analysis (TGA) were performed. Morphological features were characterized by Transmission Electron Microscopy (TEM), and Magnetic Hysteresis Measurement (VSM) analysis were performed for magnetic measurements.

Keywords: *Fe_3O_4, TEOS, PEG, chitosan, core@shell nanostructures*

Submission Date: *22 February 2021*
Acceptance Date: *13 May 2021*

**Corresponding author:* *nurdankurnazyetim@klu.edu.tr*

1. Introduction

Particles in nano size have unique properties which enable them to be used in novel applications as key figure [1]. Nanoparticles are often accepted in a special size range which is between bulk and atomic matter [2,3]. In such a size range, the properties of the nanoparticles alter with their size since surface area/volume ratio becomes prominent factor. Beside the size, the shape also affects and defines the characteristics and properties of the nanoparticles. Therefore, different groups try to produce nanoparticles in various shapes. Metallic nanoparticles can be used different applications such as sensors, catalytic applications, supercapacitors, medical applications, etc [4–11]. Among those, magnetic nanoparticles (MNPs) attract the attention of different researchers since they have vast area of application. MNPs are useful and important nanostructures since they have unique properties such as magnetic susceptibility, biocompatibility with highly stable structure [10,12]. Due to their magnetic characteristics, these nanoparticles are commonly used in various medical application such as MR imaging, drug delivery, gen delivery, protein and enzyme immobilization, cancer hyperthermia and vast amount of biomedical application [10,13–17]. MNPs can help to diagnose and treat different diseases such as cancer, cardiovascular diseases, etc [12,18,19]. MNPs are crucial since they have low toxicity, increased drug half-life [20]. Iron oxide nanoparticles exhibit superparamagnetic characteristics which are affected from oxidation [21–24]. Therefore, a shell layer is produced to cover nanoparticle from oxidation [24,25]. Such shells not only protect the MNPs but also can be used to alter the magnetic properties of nanoparticles. Such shells can also be used to functionalize the nanoparticles which give them multirole and enable them to be used in various applications [10,14–16] where more useful and functional nanostructure were obtained. Nowadays, different types of nanocomposites were produced using double and triple compound as ingredient [26–28]. Magnetic materials like Fe_3O_4 were often used in the production to give magnetic properties to the produced material or enhance the intrinsic

magnetic characteristics of the nanomaterials. Moreover, the produced magnetic material was covered with SiO_2, PEG and chitosan as cover shell where inorganic@organic core@shell nanocomposite structures were obtained [15,29–33].

Previously, similar works about organic/inorganic polymer coated Fe_3O_4 nanoparticles were reported. None of the illustrates a structure which consist of three different coating; and none of the investigates shell structure and shell size in details. In this work, the surface of Fe_3O_4 nanoparticles were coated with different inorganic/organic molecules. The effect of shell thickness and structure on morphological and magnetic properties were assessed.

2. Experimental

2.1. Materials and spectral data measurements

$FeCl_3.6H_2O$, $FeCl_2.4H_2O$, tetraethylortasilicate (TEOS), PEG-4000, chitosan (medium molecular weight), sodium oleate, glutaraldehyde 25% in H_2O, ammonia (NH_3) 28%, ethanol were purchased from Sigma-Aldrich.

Shimadzu IR Prestige 21 was used in FTIR spectrometer investigations for the wavelengths between of 400 to 4000 cm^{-1}. HR-TEM images were obtained using JEOL 1220 JEM electron microscope with an acceleration voltage of 200 kV. Magnetic measurements results were obtained at room temperature by Cryogenic Limited PPMS-vibrating sample magnetometer (VSM), with the maximum magnetic field of ± 5 Tesla. Thermogravimetric analysis of the polymeric supports was determined using LABSYS evo SETARAM Instrumentation using a 15 to 20 mg polymer sam- ple heated up to 900 °C at a rate of 10 °C/min.

2.2. Synthesis of Fe_3O_4 MNPs

Fe_3O_4 MNPs was synthesized according to previous studies [15,34]. Briefly, 25.0 mL of Fe^{3+}/Fe^{2+} mixture was prepared by dissolving 2.6 g $FeCl_3.6H_2O$ and 1.0 g $FeCl_2.4H_2O$ in a two-necked round bottom flask under N_2 atmosphere. Then the materials were completely dissolved, a 28% NH_3 solution (10 mL) was added dropwise to the reaction medium. The resulting black MNPs were collected with the help of a magnet and washed with pure water and ethyl alcohol and dried in a vacuum oven at 40 °C for 24 hours (See Fig. 1).

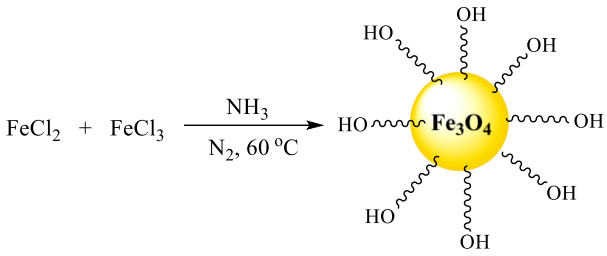

Fig.1. Synthesis scheme of Fe_3O_4 MNPs

2.3. Synthesis of Fe_3O_4 MNPs coated with inorganic / organic molecules

2.3.1. Synthesis of Fe_3O_4 MNPs coated with TEOS (Fe_3O_4@SiO_2)

0.1 g Fe_3O_4 was sonicated for 30 minutes in 20 mL ethyl alcohol. Then, 1 mL of TEOS and 1 mL of 28% NH_3 solution were added to the solution. The solution was stirred at room temperature for 12 h. MNPs were collected using a magnet. The collected precipitate was washed with purified water and ethyl alcohol. The resulting product was kept in a drying oven at 40 °C for 24 hours under vacuum conditions [15,34].

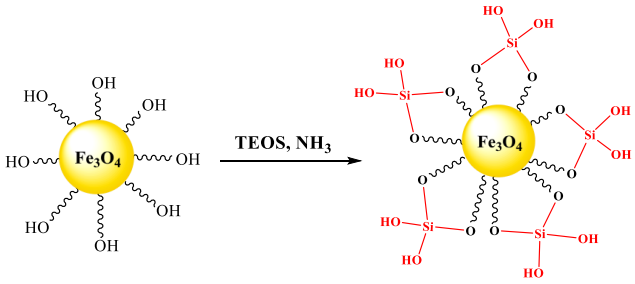

Fig.2. Schematics of the production of SiO_2 shell over Fe_3O_4 core.

2.3.2. Synthesis of Fe_3O_4 MNps coated with chitosan

In previous works, the coating of Fe_3O_4 MNPs with chitosan was performed [35]. In this report, we modified the previous techniques where glutaraldehyde was added to the recipe. 20 mL deionized water was added to 0.4 g Fe_3O_4 MNPs and sonicated for 30 minutes in an ultrasonic bath. Then, chitosan solution was added to the mixture. The chitosan solution was prepared by dissolving 1 g of chitosan in 50 mL of 1% (v/v) acetic acid solution, pH 4.0. After 1 h, glutaraldehyde solution (1 mL) was added to the solution medium. The mixture was stirred on magnetic stirrer for 12 h. Chitosan coated MNPs were collected with the help of a magnet. It was dried in a vacuum oven at 40 °C for 24 hours

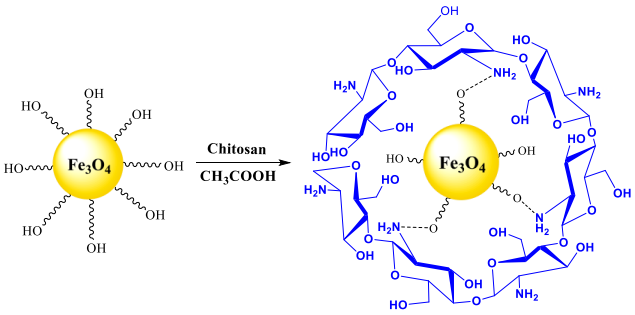

Fig.3. Schematics of the production of chitosan shell over Fe_3O_4 core.

2.3.3. Synthesis of Fe_3O_4 MNPs coated with PEG

0.1 g of Fe_3O_4 and 10 mL of distilled water were added to a 50 mL round bottom flask and sonicated in an ultrasonic bath for 20 min. Then 5 mL of sodium oleate solution was added under N_2 gas. The solution was stirred for 20 minutes. 0.25 g of PEG-4000 was dissolved in 20 ml of deionized water and added to the reaction medium. The mixture was then sonicated for 1 hour. The products were separated using magnet after cooling the suspension at room temperature. The products were dried under vacuum at 40 °C for 24 hours [36].

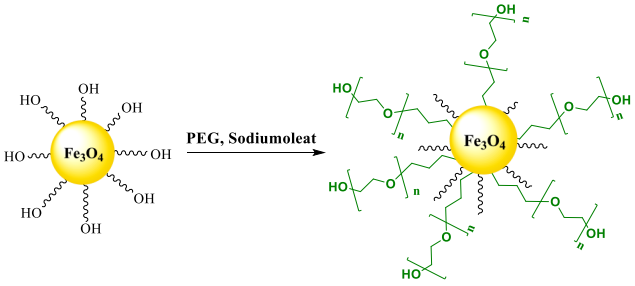

Fig.4. Schematics of the production of PEG shell over Fe_3O_4 core.

3. Results

3.1. FTIR spectrums of Fe_3O_4, Fe_3O_4@SiO_2, Fe_3O_4@PEG and Fe_3O_4@chitosan

FTIR spectra of Fe_3O_4, Fe_3O_4@SiO_2, Fe_3O_4@PEG and Fe_3O_4@chitosan MNPs are presented in Fig. 5. When the FTIR spectrum for Fe_3O_4 MNPs was examined, it was seen that the bands were observed at approximately 583 cm^{-1} and 456 cm^{-1} which belong to the internal stretching vibrations of the metal in the tetrahedral region (Fetetra↔O) and octahedral region (Feocta↔O) [37]. In the FTIR spectrum of Fe_3O_4@SiO_2 MNPs, Fe-O stretching vibration was observed at 583 cm^{-1}. After coating the nanoparticles with TEOS, the bands at 1053, 948 and 795 cm^{-1} were observed. The bands in these number of waves belong to Si-O-Si asymmetric stress vibrations [38].

In the FTIR spectrum of Fe_3O_4@PEG nanocomposite, peaks at 595 cm^{-1} were attributed to the Fe-O group. The ν(C-H) asymmetric and symmetric stretching vibration was observed at 2890 and 2930 cm^{-1}, while the ν(O-H) stretching vibration was observed at 3450 cm^{-1} [39]. C-H related bending was observed at 1485 and 1495 cm^{-1}.

The FTIR spectra of Fe_3O_4@chitosan is shown in Fig. 5. When the FTIR spectrum was examined, the peaks at around 3420 cm^{-1} were seen, they were attributed to the stretching vibration of -OH and N-H bands and two characteristic absorption bands from the Fe-O in Fe_3O_4 nanoparticles appeared at 585 cm^{-1} and 598 cm^{-1}. The absorption bands for Fe_3O_4@chitosan appeared at 2900 cm^{-1} for C-H stretching vibrations, 1690 cm^{-1} for N-H bending vibrations and 1450 cm^{-1} for C-N stretching vibrations. The weakening of the peaks for -OH and -NH_2 groups in the spectrum of chitosan coated Fe_3O_4 particles can be explained as their depletion during the binding reaction [40].

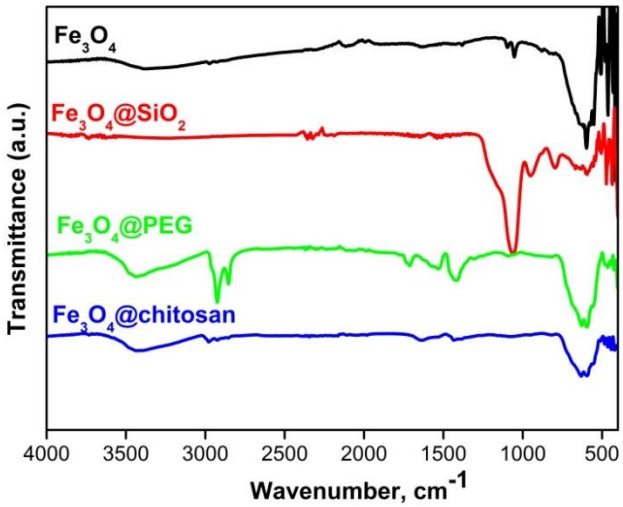

Fig.5. FTIR spectrum of Fe_3O_4, Fe_3O_4@SiO_2, Fe_3O_4@PEG, Fe_3O_4@chitosan.

3.2. TGA of Fe_3O_4, Fe_3O_4@SiO_2, Fe_3O_4@PEG and Fe_3O_4@chitosan

The TGA curves of the Fe_3O_4@SiO_2, Fe_3O_4@PEG and Fe_3O_4@chitosan hybrid materials are illustrated in Fig. 6.

Two stages of weight loss were observed in the TGA curve of the Fe_3O_4@SiO_2 nanomaterial which are 28.08-141.03°C and 144.36-287.36°C. While the adsorbed water removed, 2.416% mass loss was seen in the first step, it was thought that the main structure decomposed by 6.037% mass loss in the second step [41].

Three stages of weight loss were observed in the TGA curve of the Fe_3O_4@PEG nanomaterial which are 161.18-279.71°C (mass loss 3.658%), 281.48–515.58°C (mass loss 12.174%), and 530.14–900 °C (mass loss 22.174%). The

adsorbed water in the structure was removed in the first step, decomposition of C-C and C-O units was seen in the second step, and decomposition of O-H units was seen in the third step [42].

Three stages of weight loss were observed in the TGA curve of the Fe_3O_4@chitosan nanomaterial which were at 46.21-122.11°C, 153.90–477.98°C, and 493.64–900 °C. The first step caused 0.487% mass loss, which is due to the dehydration of the samples. 4.036% mass loss was seen in the second step, which was thought to be exist due to the breakage of C-N and C-C bonds where NH_3, CH_4 and CO units were separated from the structure. In the third step 2.588% mass loss was observed, which is thought to be caused by the breakage of N-H, C=O and C-H bonds [43].

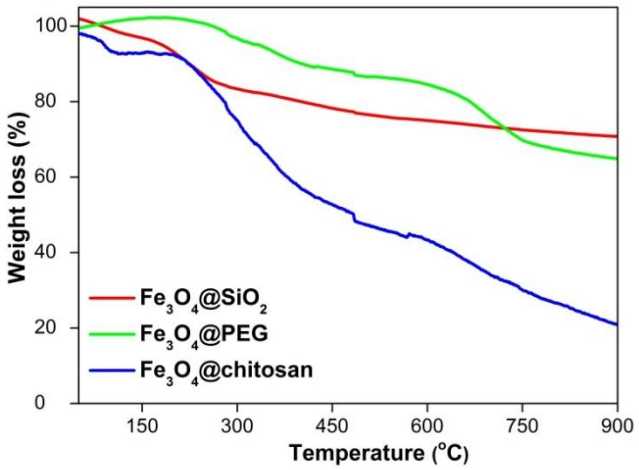

Fig.6. TGA curves of Fe_3O_4, Fe_3O_4@SiO_2, Fe_3O_4@PEG, Fe_3O_4@chitosan

3.3. TEM images of Fe_3O_4, Fe_3O_4@SiO_2, Fe_3O_4@PEG and Fe_3O_4@chitosan

Microscopic investigations of Fe_3O_4, Fe_3O_4@SiO_2, Fe_3O_4@PEG and Fe_3O_4@chitosan MNPs were performed using transmission electron microscopy (TEM) (See Fig. 7). When the TEM images of Fe_3O_4 MNPs are examined, it was seen that the nanoparticles have a typical spheric Fe_3O_4 particle structure in nano size (Fig. 7a). Magnetic nanoparticles agglomerate due to their high magnetic properties. It was seen that the Fe_3O_4 MNPs had an average diameter of about 12 nm.

It was clearly seen from the TEM image that silica coated magnetic nanoparticles have a typical core-shell structure where the magnetic core is dark, the silica shell is light (Fig. 7b). From this image, it can be said that the magnetic nanoparticles are completely and smoothly covered with a silica layer. While the core thickness for Fe_3O_4@SiO_2 was determined as approximately 99.67 nm, the shell thickness was found to be approximately 17.76 nm from the TEM image.

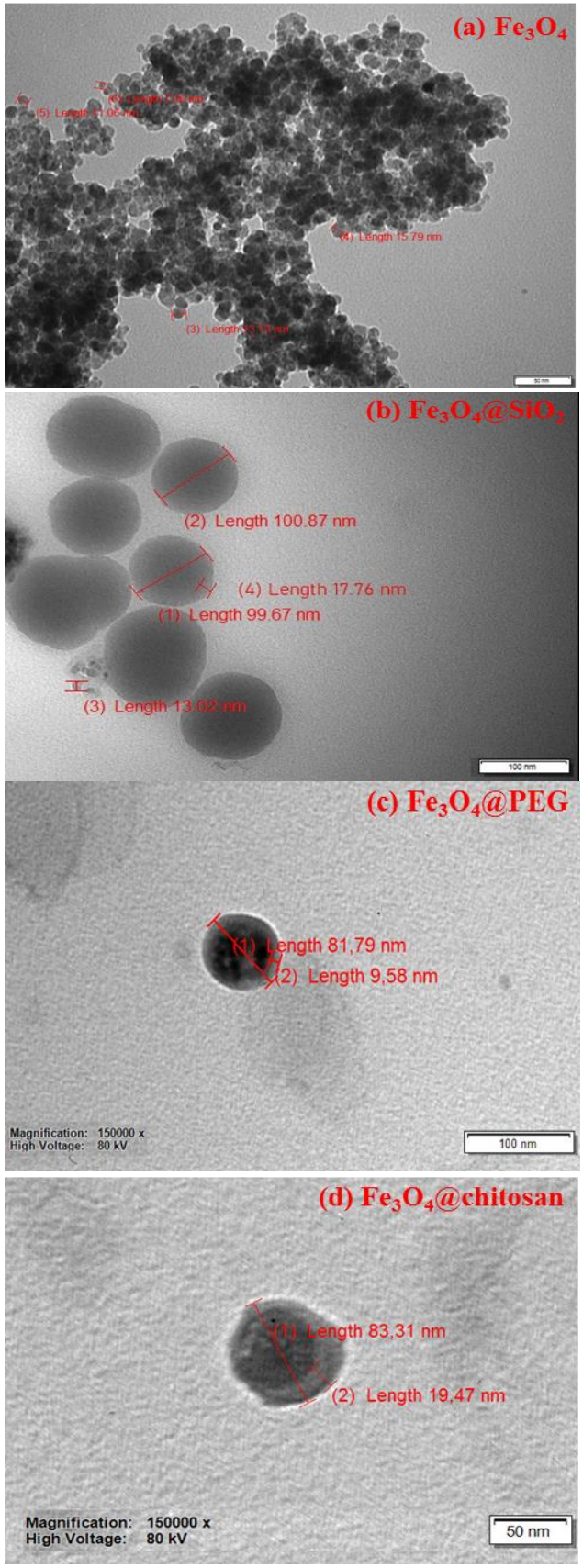

Fig.7. TEM images of **(a)** Fe_3O_4, **(b)** Fe_3O_4@SiO_2, **(c)** Fe_3O_4@PEG, **(d)** Fe_3O_4@chitosan

Fe_3O_4@PEG was illustrated in Fig. 7c. Total size of the PEGylated nanoparticle was found to be 81.79 nm with 9.58

nm. It can be identified in the image that Fe_3O_4 nanoparticles were stay in agglomerated state in the PEG shell. It was seen in the figure that some Fe_3O_4 nanoparticles around 10 nm were accumulated in the centre of the core@shell structure, but some gaps were identified. Such a case illustrate that nanoparticles are agglomeration of the Fe_3O_4 MNPs which increases the overall size of the composite.

Fe_3O_4@chitosan was illustrated in Fig. 7d. It was seen from the TEM image that the diameter of the chitosan coated Fe_3O_4 particles was approximately 83.31 nm and the shell thickness approximately 19.47 nm.

3.4. Magnetic measurement of Fe_3O_4, Fe_3O_4@SiO_2, Fe_3O_4@PEG and Fe_3O_4@chitosan MNPs

Magnetic hysteresis curves of Fe_3O_4, Fe_3O_4@SiO_2 Fe_3O_4@PEG and Fe_3O_4@chitosan are shown in Fig. 8. Room temperature specific magnetization versus applied magnetic field curve measurements of the samples indicate that nanoparticles exhibit superparamagnetic characteristics where a saturation magnetization values were seen. Saturation magnetization value for Fe_3O_4, Fe_3O_4@SiO_2 Fe_3O_4@PEG and Fe_3O_4@chitosan MNPs were found to be 63.7 emu/g, 17.3 emu/g, 49.8 emu/g and 20.4 emu/g respectively.

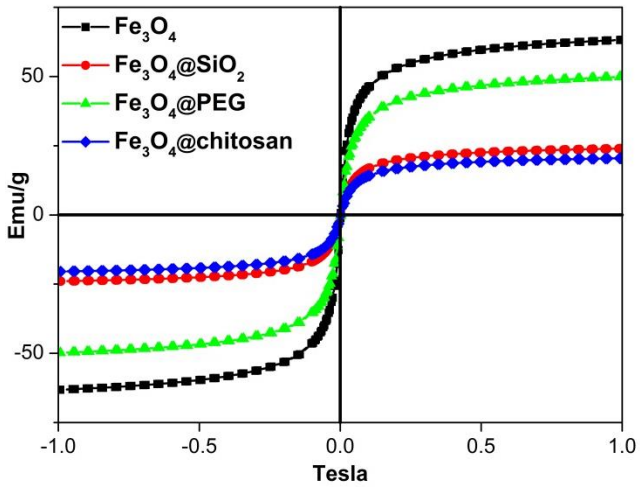

Fig.8. Magnetic hysteresis of Fe_3O_4, Fe_3O_4@SiO_2, Fe_3O_4@PEG, Fe_3O_4@chitosan

4. Conclusion

In the study, Fe_3O_4 MNPs were prepared by co-precipitation method and core-shell structures were obtained by coating with silica, PEG and chitosan. It is known that Fe_3O_4 structures show magnetic hysteresis in their magnetic investigations. In this work, our nanoparticles were investigated with VSM, it was understood that Fe_3O_4 based MNPs showed superparamagnetic like hysteresis curves. TEM images of the samples were obtained which confirmed that Fe_3O_4@SiO_2, Fe_3O_4@PEG and Fe_3O_4@chitosan MNPs are in core@shell form. Magnetic investigations revealed that covering nanoparticles with shell dramatically reduced the magnetic characteristics of the bare Fe_3O_4 nanoparticles. Core@shell structure of the Fe_3O_4@SiO_2, Fe_3O_4@PEG and Fe_3O_4@chitosan nanocomposites were also confirmed by spectroscopic analysis techniques as well.

References

[1] J. Jeevanandam, A. Barhoum, Y.S. Chan, A. Dufresne, M.K. Danquah, Review on nanoparticles and nanostructured materials: history, sources, toxicity and regulations, Beilstein J. Nanotechnol. 9 (2018) 1050–1074. doi:10.3762/bjnano.9.98.

[2] M. Singh, S. Manikandan, A.K. Kumaraguru, Nanoparticles: A New Technology with Wide Applications, Res. J. Nanosci. Nanotechnol. 1 (2011) 1–11. doi:10.3923/rjnn.2011.1.11.

[3] I. Khan, K. Saeed, I. Khan, Nanoparticles: Properties, applications and toxicities, Arab. J. Chem. 12 (2019) 908–931. doi:10.1016/j.arabjc.2017.05.011.

[4] M. İlhan, M.M. Koç, B. Coşkun, A. Dere, F. Yakuphanoğlu, Structural and optoelectronic characterization of Cu_2CoSnS_4 quaternary functional photodetectors, Optik (Stuttg). 212 (2020) 164724. doi:10.1016/j.ijleo.2020.164724.

[5] M. İlhan, M.M. Koç, B. Coşkun, M. Erkovan, F. Yakuphanoğlu, Cd dopant effect on structural and optoelectronic properties of TiO_2 solar detectors, J. Mater. Sci. Mater. Electron. 32 (2021) 2346–2365. doi:10.1007/s10854-020-05000-3.

[6] M.M.Koç, M. İlhan, Infrared Sensing Properties of Quaternary Cu_2CoSnS_4 Photodetectors, J. Mater. Electron. Devices. 1 (2020) 19–24.

[7] N. Kurnaz Yetim, N. Aslan, M.M. Koç, Structural and catalytic properties of Fe_3O_4 doped Bi_2S_3 novel magnetic nanocomposites: p-Nitrophenol case, J. Environ. Chem. Eng. 8 (2020) 104258. doi:10.1016/j.jece.2020.104258.

[8] N. Kurnaz Yetim, Catalytic Properties of Hydrothermally Synthesized Flower-like NiO@Fe_3O_4, Düzce Üniversitesi Bilim ve Teknol. Derg. 8 (2020) 1964–1974. doi:10.29130/dubited.721970.

[9] N. Kurnaz Yetim, N. Aslan, A. Sarıoğlu, N. Sarı, M.M. Koç, N.K. Yetim, N. Aslan, A. Sarıoğlu, N. Sarı, M.M. Koç, Structural, electrochemical and optical properties of hydrothermally synthesized transition metal oxide (Co_3O_4, NiO, CuO) nanoflowers, J. Mater. Sci. Mater. Electron. 31 (2020) 12238–12248. doi:10.1007/s10854-020-03769-x.

[10] N. Aslan, B. Ceylan, M.M. Koç, F. Findik, Metallic nanoparticles as X-Ray computed tomography (CT) contrast agents: A review, J. Mol. Struct. 1219 (2020) 128599.

doi:10.1016/j.molstruc.2020.128599.

[11] D. Nartop, E. Hasanoğlu Özkan, N.K. Yetim, N. Sarı, Qualitative enzymatic detection of organophosphate and carbamate insecticides, J. Environ. Sci. Heal. - Part B Pestic. Food Contam. Agric. Wastes. (2020) 951–958. doi:10.1080/03601234.2020.1797425.

[12] M. Filippousi, S.A. Papadimitriou, D.N. Bikiaris, E. Pavlidou, M. Angelakeris, D. Zamboulis, H. Tian, G. Van Tendeloo, Novel core-shell magnetic nanoparticles for Taxol encapsulation in biodegradable and biocompatible block copolymers: Preparation, characterization and release properties, Int. J. Pharm. 448 (2013) 221–230. doi:10.1016/j.ijpharm.2013.03.025.

[13] O. Veiseh, J.W. Gunn, M. Zhang, Design and fabrication of magnetic nanoparticles for targeted drug delivery and imaging, Adv. Drug Deliv. Rev. 62 (2010) 284–304. doi:10.1016/j.addr.2009.11.002.

[14] M.M. Koç, N. Aslan, A.P. Kao, A.H. Barber, Evaluation of X-ray tomography contrast agents: A review of production, protocols, and biological applications, Microsc. Res. Tech. 82 (2019). doi:10.1002/jemt.23225.

[15] N. Kurnaz Yetim, F. Kurşun Baysak, M.M. Koç, D. Nartop, Characterization of magnetic Fe_3O_4@SiO_2 nanoparticles with fluorescent properties for potential multipurpose imaging and theranostic applications, J. Mater. Sci. Mater. Electron. 31 (2020) 18278–18288. doi:10.1007/s10854-020-04375-7.

[16] R. Karaçam, N.K. Yetim, M.M. Koç, Structural and Magnetic Investigation of Bi_2S_3@Fe_3O_4 Nanocomposites for Medical Applications, J. Supercond. Nov. Magn. 33 (2020) 2715–2725. doi:10.1007/s10948-020-05518-x.

[17] E. Hasanoğlu Özkan, N. Sarı, Use of immobilized novel dendritic molecules as a marker for the detection of glucose in artificial urine, J. Mol. Struct. 1201 (2020) 127134. doi:10.1016/j.molstruc.2019.127134.

[18] C. Binns, P. Prieto, S. Baker, P. Howes, R. Dondi, G. Burley, L. Lari, R. Kröger, A. Pratt, S. Aktas, J.K. Mellon, Preparation of hydrosol suspensions of elemental and core-shell nanoparticles by co-deposition with water vapour from the gas-phase in ultra-high vacuum conditions, J. Nanoparticle Res. 14 (2012) 1136. doi:10.1007/s11051-012-1136-6.

[19] M.M. Yallapu, S.P. Foy, T.K. Jain, V. Labhasetwar, PEG-functionalized magnetic nanoparticles for drug delivery and magnetic resonance imaging applications, Pharm. Res. 27 (2010) 2283–2295. doi:10.1007/s11095-010-0260-1.

[20] A. Hervault, N.T.K. Thanh, Magnetic nanoparticle-based therapeutic agents for thermo-chemotherapy treatment of cancer, Nanoscale. 6 (2014) 11553–11573. doi:10.1039/c4nr03482a.

[21] S. Aktas, S.C. Thornton, C. Binns, L. Lari, A. Pratt, R. Kröger, M.A. Horsfield, Control of gas phase nanoparticle shape and its effect on MRI relaxivity, Mater. Res. Express. 2 (2015) 105356. doi:10.1088/2053-1591/2/3/035002.

[22] S. Aktas, S.C. Thornton, C. Binns, P. Denby, Gas phase synthesis of core-shell Fe@FeO x magnetic nanoparticles into fluids, J. Nanoparticle Res. 118 (2016) 365. doi:10.1007/s11051-016-3659-8.

[23] H. Shao, C. Min, D. Issadore, M. Liong, T.J. Yoon, R. Weissleder, H. Lee, Magnetic nanoparticles and micronmr for diagnostic applications, Theranostics. 2 (2012) 55–65. doi:10.7150/thno.3465.

[24] F. Sahin, E. Turan, H. Tumturk, G. Demirel, Core-shell magnetic nanoparticles: A comparative study based on silica and polydopamine coating for magnetic bio-separation platforms, Analyst. 137 (2012) 5654–5658. doi:10.1039/c2an36211b.

[25] H. Tumturk, F. Sahin, E. Turan, Magnetic nanoparticles coated with different shells for biorecognition: High specific binding capacity, Analyst. 139 (2014) 1093–1100. doi:10.1039/c3an01726e.

[26] T.T.T. Mai, P.T. Ha, H.N. Pham, T.T.H. Le, H.L. Pham, T.B.H. Phan, D.L. Tran, X.P. Nguyen, Chitosan and O-carboxymethyl chitosan modified Fe_3O_4 for hyperthermic treatment, Adv. Nat. Sci. Nanosci. Nanotechnol. 3 (2012) 5. doi:10.1088/2043-6262/3/1/015006.

[27] J. Safaei-Ghomi, F. Eshteghal, H. Shahbazi-Alavi, A facile one-pot ultrasound assisted for an efficient synthesis of benzo[g]chromenes using Fe_3O_4/polyethylene glycol (PEG) core/shell nanoparticles, Ultrason. Sonochem. 33 (2016) 99–105. doi:10.1016/j.ultsonch.2016.04.025.

[28] P. Nehra, R.P. Chauhan, N. Garg, K. Verma, Antibacterial and antifungal activity of chitosan coated iron oxide nanoparticles, Br. J. Biomed. Sci. 75 (2018) 13–18. doi:10.1080/09674845.2017.1347362.

[29] S. Zinadini, A.A. Zinatizadeh, M. Rahimi, V. Vatanpour, H. Zangeneh, M. Beygzadeh, Novel high flux antifouling nanofiltration membranes for dye removal containing carboxymethyl chitosan coated Fe_3O_4 nanoparticles, Desalination. 349 (2014) 145–154. doi:10.1016/j.desal.2014.07.007.

[30] T. Saravanakumar, T. Palvannan, D.H. Kim, S.M. Park, Optimized immobilization of peracetic acid producing recombinant acetyl xylan esterase on chitosan coated-Fe_3O_4 magnetic nanoparticles, Process Biochem. 49 (2014) 1920–1928. doi:10.1016/j.procbio.2014.08.008.

[31] M. V. Avdeev, A. V. Feoktystov, P. Kopcansky, G. Lancz, V.M. Garamus, R. Willumeit, M. Timko, M. Koneracka, V. Zavisova, N. Tomasovicova, A. Jurikova, K. Csach, L.A. Bulavin, Structure of water-based ferrofluids with sodium oleate and polyethylene glycol stabilization by small-angle neutron scattering: Contrast-variation experiments, J. Appl. Crystallogr. 43 (2010) 959–969. doi:10.1107/S0021889810025379.

[32] M. Anbarasu, M. Anandan, E. Chinnasamy, V. Gopinath, K. Balamurugan, Synthesis and

characterization of polyethylene glycol (PEG) coated Fe_3O_4 nanoparticles by chemical co-precipitation method for biomedical applications, Spectrochim. Acta - Part A Mol. Biomol. Spectrosc. 135 (2015) 536–539. doi:10.1016/j.saa.2014.07.059.

[33] I. Dayana, T. Sembiring, A.P. Tetuko, K. Sembiring, N. Maulida, Z. Cahyarani, E.A. Setiadi, N.S. Asri, M. Ginting, P. Sebayang, The effect of tetraethyl orthosilicate (TEOS) additions as silica precursors on the magnetite nano-particles (Fe_3O_4) properties for the application of ferro-lubricant, J. Mol. Liq. 294 (2019) 111557. doi:10.1016/j.molliq.2019.111557.

[34] N. Kurnaz Yetim, F. Kurşun Baysak, M.M. Koç, D. Nartop, Synthesis and characterization of Au and Bi_2O_3 decorated Fe_3O_4@PAMAM dendrimer nanocomposites for medical applications, J. Nanostructure Chem. (2021) 1–11. doi:10.1007/s40097-021-00386-w.

[35] M.J. Chaichi, M. Ehsani, A novel glucose sensor based on immobilization of glucose oxidase on the chitosan-coated Fe_3O_4 nanoparticles and the luminol-H_2O_2-gold nanoparticle chemiluminescence detection system, Sensors Actuators, B Chem. 223 (2016) 713–722. doi:10.1016/j.snb.2015.09.125.

[36] J. Safaei-Ghomi, F. Eshteghal, Nano-Fe_3O_4/PEG/succinic anhydride: A novel and efficient catalyst for the synthesis of benzoxanthenes under ultrasonic irradiation, Ultrason. Sonochem. 38 (2017) 488–495. doi:10.1016/j.ultsonch.2017.03.047.

[37] H. Rashidi Nodeh, W.A. Wan Ibrahim, I. Ali, M.M. Sanagi, Development of magnetic graphene oxide adsorbent for the removal and preconcentration of As(III) and As(V) species from environmental water samples, Environ. Sci. Pollut. Res. 23 (2016) 9759–9773. doi:10.1007/s11356-016-6137-z.

[38] L. Sun, S. Hu, H. Sun, H. Guo, H. Zhu, M. Liu, H. Sun, Malachite green adsorption onto Fe3O4@SiO2-NH2: Isotherms, kinetic and process optimization, RSC Adv. 5 (2015) 11837–11844. doi:10.1039/c4ra13402h.

[39] K. Shameli, M. Bin Ahmad, S.D. Jazayeri, S. Sedaghat, P. Shabanzadeh, H. Jahangirian, M. Mahdavi, Y. Abdollahi, Synthesis and characterization of polyethylene glycol mediated silver nanoparticles by the green method, Int. J. Mol. Sci. 13 (2012) 6639–6650. doi:10.3390/ijms13066639.

[40] Y. Osuna, K.M. Gregorio-Jauregui, J.G. Gaona-Lozano, I.M. De La Garza-Rodríguez, A. Ilyna, E.D. Barriga-Castro, H. Saade, R.G. López, Chitosan-coated magnetic nanoparticles with low chitosan content prepared in one-step, J. Nanomater. 2012 (2012) 7. doi:10.1155/2012/327562.

[41] R. Abu-Reziq, H. Alper, D. Wang, M.L. Post, Metal supported on dendronized magnetic nanoparticles: Highly selective hydroformylation catalysts, J. Am. Chem. Soc. 128 (2006) 5279–5282. doi:10.1021/ja060140u.

[42] B. Feng, R.Y. Hong, L.S. Wang, L. Guo, H.Z. Li, J. Ding, Y. Zheng, D.G. Wei, Synthesis of Fe_3O_4/APTES/PEG diacid functionalized magnetic nanoparticles for MR imaging, Colloids Surfaces A Physicochem. Eng. Asp. 328 (2008) 52–59. doi:10.1016/j.colsurfa.2008.06.024.

[43] M.A. Zulfikar, S. Afrita, D. Wahyuningrum, M. Ledyastuti, Preparation of Fe_3O_4-chitosan hybrid nano-particles used for humic acid adsorption, Environ. Nanotechnology, Monit. Manag. 6 (2016) 64–75. doi:10.1016/j.enmm.2016.06.001.